An Exact Solution to Steady Heat Conduction in a Two-Dimensional Annulus on a One-Dimensional Fin: Application to Frosted Heat Exchangers With Round Tubes

A. D. Sommers
Graduate Research Assistant
e-mail: asommers@uiuc.edu

A. M. Jacobi
Professor of Mechanical Engineering
e-mail: a-jacobi@uiuc.edu

Department of Mechanical and Industrial Engineering,
University of Illinois,
1206 West Green Street,
Urbana, IL 61801

The fin efficiency of a high-thermal-conductivity substrate coated with a low-thermal-conductivity layer is considered, and an analytical solution is presented and compared to alternative approaches for calculating fin efficiency. This model is appropriate for frost formation on a round-tube-and-fin metallic heat exchanger, and the problem can be cast as conduction in a composite two-dimensional circular cylinder on a one-dimensional radial fin. The analytical solution gives rise to an eigenvalue problem with an unusual orthogonality condition. A one-term approximation to this new analytical solution provides fin efficiency calculations of engineering accuracy for a range of conditions, including most frosted-coated metal fins. The series solution and the one-term approximation are of sufficient generality to be useful for other cases of a low-thermal-conductivity coating on a high-thermal-conductivity substrate. [DOI: 10.1115/1.2165210]

Keywords: frost, fin efficiency, conduction, sector method, heat transfer

Introduction

Xia and Jacobi [1] presented the solution to heat conduction in a two-dimensional slab on a one-dimensional straight fin, and using a numerical solution to the fully two-dimensional problem they identified the parameter space for which that simplified model is appropriate. Moreover, they applied this heat transfer model to frost growth on a straight metallic fin, typical to a flat-tube heat exchanger operating under frosting conditions. However, most heat exchangers operating under frosted-surface conditions are constructed with plain fins and round tubes. The analytical solution presented for the straight fin is not valid for the round-tube geometry.

For round-tube heat exchangers, the so-called sector method is often used. In this method, the fin surface is divided into hexagonal or rectangular regions around each tube, and circular sectors are fit to the geometric profile of the selected region. Typically, these regions are subdivided into eight zones and then further divided into sectors as shown in Fig. 1. The radius of each edge of the sector is approximated according to the hexagonal pattern and then used to calculate the radius ratio and surface area of each sector, RR_n and S_n, respectively. The overall fin efficiency is found by summing the product of the individual efficiencies and surface areas for each sector and dividing by the total surface area of the eight zones. This method is based on the assumptions of radial conduction in each sector and an adiabatic tip for each sector. Thus, the widely used sector method—a method used for complicated fin-and-tube heat exchangers—has the efficiency of a circular fin as its basis. The well-known expression for circular fin efficiency involves Bessel functions, and in 1949 Schmidt [2] provided an approximation to this expression in terms of the hyperbolic tangent function. This solution is still used by some engineers today when calculating fin efficiency by the sector method. The application of the sector method to various round-tube-and-fin geometries is detailed in the Appendix.

Under condensing or frosting conditions the fin efficiency calculation must account for sensible and latent heat effects. A common practice is to include an additional source term in the fin heat diffusion equation for the latent heat due to mass transfer along the surface. In this approach, the final form of the governing differential equation is the same as for dry-surface conditions, but it includes two dependent variables: θ, the nondimensional temperature difference, and W_s, the humidity ratio at the surface of the fin. For condensing conditions, McQuiston [3] assumed $(W_a\text{-}W_s)$ to be linearly related to $(T_a\text{-}T_s)$ and in this way eliminated one of the dependent variables. However, this ad hoc approximation requires a priori knowledge of the temperature range, in order to evaluate the constant of proportionality between humidity ratio and temperature. Wu and Bong [4] improved upon this idea by using a psychrometric relationship between the humidity ratio of saturated air at the surface, W_s, and T_s. When the difference between the fin base temperature and the fin tip temperature is small, this assumption is excellent, and the relationship is linear and thermodynamically known. However, Wu and Bong developed their approach for wet fins and not frosted fins, and therefore their method does not account for the effect that a frost conduction resistance has on the fin efficiency. In a similar study of fin efficiency under condensing conditions, Hong and Webb [5] suggested a modification to the Schmidt solution that more accurately approximates the Bessel function solution; they then followed the approach of McQuiston [3] in deriving a wet fin efficiency solution and pointed out that for high-humidity conditions the difference between the dry-surface fin efficiency and the wet-surface fin efficiency can be as high as 35%.

In a paper on frosted coil performance, Mago and Sherif [6] computed the fin efficiency of a frosted rectangular fin using an equivalent circular area. In order to account for frost, they included the mass transfer effects in defining the air-side convective

Contributed by the Heat Transfer Division of ASME for publication in the JOURNAL OF HEAT TRANSFER. Manuscript received May 19, 2005; final manuscript received August 31, 2005. Review conducted by A. Haji-Sheikh.

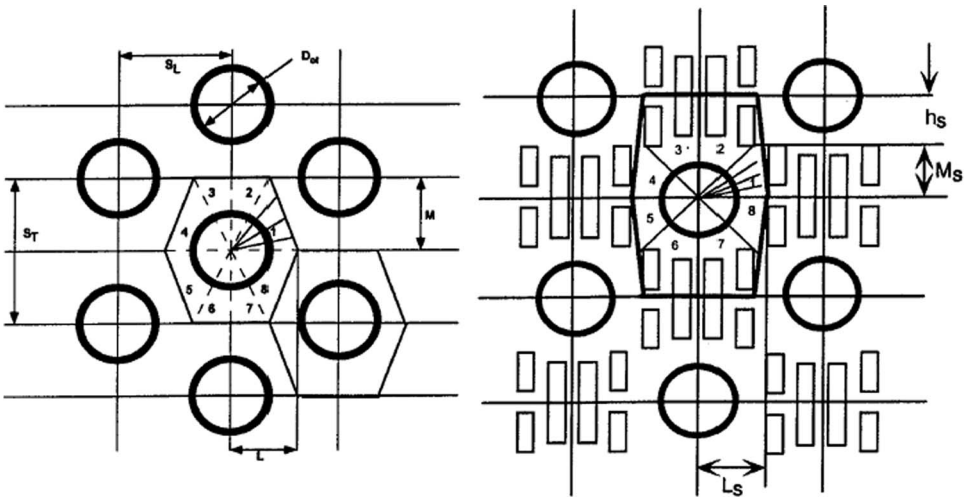

Fig. 1 Two different examples of the hexagonal pattern that emerges when using the sector method [9]

coefficient and defined the fin efficiency in terms of enthalpies rather than temperatures. Their method, however, neglects conduction in the frost layer and requires knowledge about the slope of the saturated enthalpy-temperature curve evaluated at the frost surface temperature. In a paper on pin-fin heat exchangers, Kondepudi and O'Neal [7] calculated fin efficiency using a modified fin parameter, m, to account for the frost conduction resistance. They found that the presence of a 1-mm-thick frost layer on the fin can reduce the fin efficiency by as much as 10% in comparison to the dry, unfrosted fin. Their analysis, however, assumes one-dimensional conduction in the frost layer and uses the hyperbolic tangent function as a simplification to the modified-Bessel solution.

There have been a number of related papers on heat conduction in composite slabs, as reviewed by Xia and Jacobi [1]. The current study extends that earlier research and is motivated by a desire for a convenient expression for fin efficiency that accounts for the frost conduction resistance and latent heat effects and is appropriate for operating conditions typical to refrigeration and heat pumping systems. In this paper, we consider an annular conduction domain and develop expressions for the fin efficiency of circular fins; the results of which can be used directly or in conjunction with the sector method.

Problem Formulation

The physical situation of interest, frost on a metallic fin, is shown in Fig. 2 for a round-tube heat exchanger with constant-thickness fins. Assuming a uniform convection coefficient, conduction in the ϕ-direction is neglected due to symmetry, and a two-dimensional analysis will be performed. As shown by Xia and Jacobi [1], for cases where $\mathrm{Bi} > 0.05$ and $\psi < 0.1$, this assumption is valid, and the fin can be approximated as one-dimensional with a two-dimensional coating. This situation represents the parametric range of most importance for frost on a metallic fin. The following assumptions will also be invoked: steady-state, no internal generation, and constant thermophysical properties. The frost layer is assumed to be of uniform thickness, and zero contact resistance is assumed between the fin and the frost. The convection coefficient, free-stream temperature, and base temperature considered in this analysis are fixed and assumed to be known. With these assumptions, the fin temperature is a function of r only (i.e., $T_1(r)$), and the temperature within the frost layer is a function of r and z (i.e., $T_2(r,z)$).

The governing equation for the temperature distribution along the fin, material 1, is

$$\frac{k_1 t}{r}\frac{d}{dr}\left(r\frac{dT_1}{dr}\right) + k_2 \left.\frac{\partial T_2}{\partial z}\right|_{z=0} = 0 \quad \text{in } R_1 < r < R_2 \tag{1}$$

The heat diffusion equation in the frost layer, material 2, is

$$\frac{1}{r}\frac{\partial}{\partial r}\left(r\frac{\partial T_2}{\partial r}\right) + \frac{\partial^2 T_2}{\partial z^2} = 0 \quad \text{in } R_1 < r < R_2,\ 0 < z < \delta \tag{2}$$

Equations (1) and (2) are subject to the boundary conditions

$$\left.\frac{dT_1}{dr}\right|_{r=R_2} = 0, \qquad \left.\frac{\partial T_2}{\partial r}\right|_{r=R_2} = 0 \tag{3a}$$

$$T_1(R_1) = T_b \quad T_2(R_1, z) = T_b \tag{3b}$$

$$T_1(r) = T_2(r,0) \tag{3c}$$

$$\left.\frac{\partial T_2}{\partial z}\right|_{z=\delta} = \frac{h}{k_2}(T_\infty - T_2(r,\delta)) \tag{3d}$$

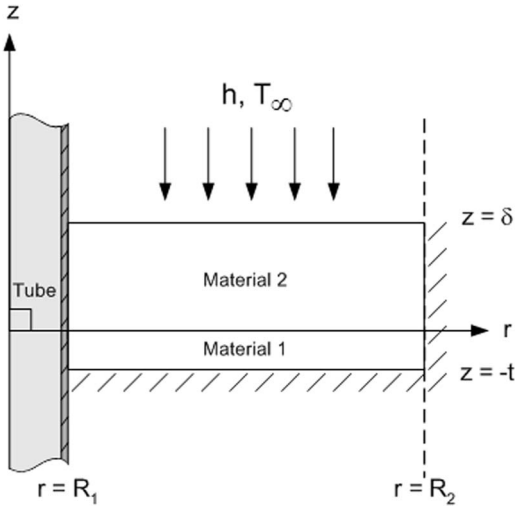

Fig. 2 Schematic of the composite slab, with the one-dimensional fin (material 1) and the two-dimensional frost layer (material 2)

Substituting Eq. (3*c*) into Eq. (1), we arrive at the following four boundary conditions for $T_2(r,z)$

$$\left.\frac{\partial T_2}{\partial r}\right|_{r=R_2}=0 \tag{4a}$$

$$T_2(R_1,z)=T_b \tag{4b}$$

$$\frac{k_1 t}{r}\frac{d}{dr}\left(r\frac{dT_2}{dr}\right)\bigg|_{z=0}+k_2\left.\frac{\partial T_2}{\partial z}\right|_{z=0}=0 \tag{4c}$$

$$\left.\frac{\partial T_2}{\partial z}\right|_{z=\delta}=\frac{h}{k_2}(T_\infty-T_2(r,\delta)) \tag{4d}$$

Now, we define the following nondimensional variables

$$\theta=\frac{T_2-T_\infty}{T_b-T_\infty}\quad r^*=\frac{r}{R_2}\quad z^*=\frac{z}{\delta} \tag{5}$$

Substituting, the boundary value problem for $T_2(r,z)$ becomes

$$\frac{1}{r^*}\frac{\partial}{\partial r^*}\left(r^*\frac{\partial\theta}{\partial r^*}\right)+\left(\frac{R_2}{\delta}\right)^2\frac{\partial^2\theta}{\partial z^{*2}}=0 \tag{6}$$

with

$$\frac{\partial\theta}{\partial r^*}=0\quad \text{at } r^*=1 \tag{7a}$$

$$\theta=1\quad \text{at } r^*=\frac{R_1}{R_2} \tag{7b}$$

$$\frac{k_1 t}{r^* R_2^2}\frac{d}{dr^*}\left(r^*\frac{d\theta}{dr}\right)+\frac{k_2}{\delta}\frac{\partial\theta}{\partial z^*}=0\quad \text{at } z^*=0 \tag{7c}$$

$$\frac{\partial\theta}{\partial z^*}+\frac{h\delta}{k_2}\theta=0\quad \text{at } z^*=1 \tag{7d}$$

Please note that from this point forward, the asterisk superscript will be dropped from the spatial coordinates for convenience, with the r and z variables taken as dimensionless unless otherwise stated. It should also be noted that the boundary condition (7*b*) conflicts with (7*d*) at location $(r,z)=(0,1)$. To resolve this conflict, the singularity was removed by replacing boundary condition (7*b*) with the following at $r=0$

$$\theta=f(z)=\begin{cases}1 & 0\leqslant z<(1-\varepsilon)\\ 1-\dfrac{[z-(1-\varepsilon)]^2}{[(2\varepsilon k_2/h\delta)+\varepsilon^2]} & (1-\varepsilon)\leqslant z\leqslant 1\end{cases} \tag{7e}$$

where $0<\varepsilon\ll 1$. We now have

$$\left.\frac{\partial\theta}{\partial z}\right|_{(0,1)}+\left.\frac{h\delta}{k_2}\theta\right|_{(0,1)}=0 \tag{8}$$

and it can be seen that Eq. (7*e*) $\rightarrow$ Eq. (7*b*) as $\varepsilon\rightarrow 0$. Perhaps more important, $f(z)$ is twice-differentiable on $0\leqslant z\leqslant 1$, and only one non-homogeneous boundary condition remains.

Therefore, separation of variables is pursued. We assume $\theta(r,z)=R(r)Z(z)$ which yields

$$\frac{1}{RM^2}\left[\frac{1}{r}\frac{dR}{dr}+\frac{d^2R}{dr^2}\right]=\frac{1}{Z}\left[-\frac{d^2Z}{dz^2}\right]=\beta_m^2 \tag{9}$$

where $M^2=(R_2/\delta)^2$. Accordingly, $R(r)$ should satisfy

$$\frac{d^2R_0}{dr^2}+\frac{1}{r}\frac{dR_0}{dr}-\beta_m^2M^2R_0=0\quad \text{in } 1<r<(R_1/R_2) \tag{10}$$

$$\text{with}\quad R_0'=0\quad \text{at } r=1 \tag{11}$$

where the subscript zero denotes no ϕ-dependence. Similarly, $Z(z)$ must satisfy

$$\frac{d^2Z}{dz^2}+\beta_m^2Z=0\quad \text{in } 0<z<1 \tag{12}$$

with

$$Z'+\frac{h\delta}{k_2}Z=0\quad \text{at } z=1 \tag{13}$$

$$\frac{k_1 t}{R_2^2}\left[R_0''Z+\frac{R_0'}{r}Z\right]+\frac{k_2}{\delta}RZ'=0\quad \text{at } z=0 \tag{14}$$

Substituting Eq. (10) into Eq. (14), the last boundary condition can be rewritten as

$$Z'+N\beta_m^2Z=0\quad \text{at } z=0 \tag{15a}$$

where

$$N=\frac{k_1 t}{\delta k_2} \tag{15b}$$

The second-order differential equations for $R(r)$ and $Z(z)$ are solved, and three of the four constants are determined using boundary condition equations (11) and (13), and (15). The eigenfunctions are

$$R_0=C_1\gamma_m[K_0(\gamma_m r)I_1(\gamma_m)-K_1(\gamma_m)I_0(\gamma_m r)] \tag{16}$$

$$Z=C_2\left[\frac{k_2}{h\delta}\beta_m\cos\beta_m(1-z)+\sin\beta_m(1-z)\right] \tag{17}$$

noting that $\gamma_m^2=\beta_m^2M^2$. The solution is thus

$$\theta(r,z)=\sum_{m=1}^{\infty}C_m\gamma_m\left[\frac{k_2}{h\delta}\beta_m\cos\beta_m(1-z)+\sin\beta_m(1-z)\right]\cdot[K_0(\gamma_m r)I_1(\gamma_m)+K_1(\gamma_m)I_0(\gamma_m r)] \tag{18}$$

where the eigenvalues β_m satisfy the following eigencondition

$$\tan(\beta_m)=\frac{\left[1-\left(\dfrac{k_1 t}{h}\right)\left(\dfrac{\beta_m}{\delta}\right)^2\right]}{\left[\dfrac{k_2}{h\delta}\beta_m+\dfrac{k_1 t}{\delta k_2}\beta_m\right]}\quad n=1,2,3,\ldots \tag{19}$$

The last boundary condition (7*b*) yields

$$f(z)=\sum_{m=1}^{\infty}C_m\gamma_m\left[\frac{k_2}{h\delta}\beta_m\cos\beta_m(1-z)+\sin\beta_m(1-z)\right]\cdot\left[K_0\left(\gamma_m\frac{R_1}{R_2}\right)I_1(\gamma_m)+K_1(\gamma_m)I_0\left(\gamma_m\frac{R_1}{R_2}\right)\right] \tag{20}$$

Now from Eq. (12), it can be shown that

$$\int_0^1 Z_n Z_m dz = \frac{1}{\beta_m^2 - \beta_n^2}\int_0^1 (Z_n'' Z_m - Z_m'' Z_n)dz \tag{21}$$

Integrating by parts and applying boundary conditions, Eqs. (13) and (15*a*), it follows

$$\int_0^1 Z_n Z_m dz = \frac{1}{\beta_m^2 - \beta_n^2}[Z_n' Z_m - Z_m' Z_n]_0^1 = -N(Z_n Z_m)_{z=0} \tag{22}$$

Thus,

$$\int_0^1 Z_n Z_m dz + N(Z_n Z_m)_{z=0} = 0 \text{ for } n \neq m \tag{23}$$

Equation (23) is needed to determine C_m; first Eq. (20) must be multiplied on both sides by Z_n and integrated from zero to one. The term $N(Z_n Z_m)_{z=0}$ is then added and subtracted from each integral, and using Eq. (23) and the fact that $f(0) = \Sigma\ C_m\ \gamma_m\ Z_m(0) R_0$, an expression for C_m is obtained. (A general derivation of Eq. (24) was provided by Xia and Jacobi [1].)

$$C_m = \frac{\displaystyle\int_0^1 f(z')Z(\beta_m;z')dz' + Nf(0)Z(\beta_m;0)}{\gamma_m R_0\left(\gamma_m; r = \frac{R_1}{R_2}\right)\left\{\displaystyle\int_0^1 [Z(\beta_m;z')]^2 dz' + N[Z(\beta_m;0)]^2\right\}} \tag{24}$$

where as $\varepsilon \to 0$

$$C_m = \frac{\displaystyle\int_0^1 Z(\beta_m;z')dz' + NZ(\beta_m;0)}{\gamma_m R_0\left(\gamma_m; r = \frac{R_1}{R_2}\right)\left\{\displaystyle\int_0^1 [Z(\beta_m;z')]^2 dz' + N[Z(\beta_m;0)]^2\right\}} \tag{25}$$

Thus finally,

$$C_m = \frac{\dfrac{1}{\beta_m} + \left(\dfrac{\beta_m k_1 t}{\delta^2 h} - \dfrac{1}{\beta_m}\right)\cos(\beta_m) + \dfrac{(k_2^2 + h k_1 t)}{\delta h k_2}\sin(\beta_m)}{\gamma_m R_0\left\{\displaystyle\int_0^1 [Z(\beta_m;z')]^2 dz' + N[Z(\beta_m;0)]^2\right\}} \tag{26a}$$

where

$$R_0 = \left[K_0\left(\gamma_m \frac{R_1}{R_2}\right)I_1(\gamma_m) + K_1(\gamma_m)I_0\left(\gamma_m \frac{R_1}{R_2}\right)\right] \tag{26b}$$

$$\int_0^1 [Z(\beta_m;z')]^2 dz' = \frac{1}{2} + \frac{k_2}{h\delta}\sin^2(\beta_m) - \frac{1}{4\beta_m}\sin(2\beta_m) + \frac{\beta_m k_2^2}{4h^2\delta^2}(2\beta_m + \sin(2\beta_m)) \tag{26c}$$

$$N[Z(\beta_m;0)]^2 = \frac{k_1 t}{h^2\delta^3 k_2}[k_2\beta_m\cos(\beta_m) + h\delta\sin(\beta_m)]^2 \tag{26d}$$

Finally, the temperature distribution inside the two-dimensional frost layer using dimensional variables is

$$\frac{T_2(r,z) - T_\infty}{T_b - T_\infty} = \sum_{m=1}^{\infty} C_m\beta_m M\left[\beta_m\left(\frac{k_2}{h\delta}\right)\cos\beta_m\left(1 - \frac{z}{\delta}\right) + \sin\beta_m\left(1 - \frac{z}{\delta}\right)\right] \cdot \left[K_0\left(\beta_m\frac{r}{\delta}\right)I_1(M\beta_m) + K_1(M\beta_m)I_0\left(\beta_m\frac{r}{\delta}\right)\right] \tag{27}$$

where β_m and C_m are given by Eqs. (19) and (26*a*)–(26*d*), respectively. The expression for the temperature along the one-dimensional fin is obtained by evaluating Eq. (27) at $z=0$ which yields

$$\frac{T_1(r) - T_\infty}{T_b - T_\infty} = \sum_{m=1}^{\infty} C_m\beta_m M\left[\beta_m\left(\frac{k_2}{h\delta}\right)\cos\beta_m + \sin\beta_m\right] \cdot \left[K_0\left(\beta_m\frac{r}{\delta}\right)I_1(M\beta_m) + K_1(M\beta_m)I_0\left(\beta_m\frac{r}{\delta}\right)\right] \tag{28}$$

The conduction heat transfer through the fin is found by differentiating Eq. (28) and using Fourier's law at $r=R_1$. Similarly, the heat flowing through the frost layer is found by differentiating Eq. (27), applying Fourier's law at $r=R_1$, and then integrating from $z=0$ to $z=\delta$. Finally, the fin efficiency is calculated by dividing the fin heat transfer rate by the maximum heat transfer rate which would exist were the entire frost surface at the base temperature, T_b. This calculation yields

$$\eta_f = \frac{2R_1}{(R_2^2 - R_1^2)h}\sum_{m=1}^{\infty} C_m\left(\frac{\beta_m}{\delta}\right)^2 R_2\left[I_1\left(\beta_m\frac{R_2}{\delta}\right)K_1\left(\beta_m\frac{R_1}{\delta}\right) - I_1\left(\beta_m\frac{R_1}{\delta}\right)K_1\left(\beta_m\frac{R_2}{\delta}\right)\right] \cdot \left\{k_1 t\beta_m\left(\frac{k_2}{h\delta}\right)\cos\beta_m + k_1 t\sin\beta_m + \frac{k_2\delta^2}{\beta_m} + \frac{k_2^2\delta}{h}\sin\beta_m - \frac{k_2\delta^2}{\beta_m}\cos\beta_m\right\} \tag{29}$$

The series solution to the fin efficiency using four terms (i.e., $m=4$) is shown in Fig. 3 for two different values of the convection coefficient, $h=20$ W m^{-2} K^{-1} and $h=40$ W m^{-2} K^{-1}, for a range of frost thicknesses. These results were obtained using Eqs. (19), (26), and (29) as well as the geometric parameters detailed in Table 1. The sector method was chosen to approximate the heat flow in a rectangular-plate fin of repeating hexagonal regions. Each of the eight zones was subdivided into fourteen sectors to ensure a high degree of numerical accuracy. It should be noted that while the fin efficiency depends on t, δ, R_1, R_2, h, k_1, and k_2, it does not depend on the temperatures T_∞ and T_b The fin efficiency does not go to unity for a frost layer of zero thickness because the metallic substrate used in the example is not a perfect conductor of heat. Furthermore, as the frost thickness approaches zero thickness, the analytical solution yields the fin efficiency as predicted by Schmidt's [2] sector method solution for dry fins to within 1%. It should also be noted that the error that would have occurred had conduction through the frost layer been neglected could be as high as 18% for the conditions used in this example, and this error would be more pronounced for thicker frost layers. This finding emphasizes the need for including these effects and suggests that an expression which properly accounts for conduction through both the frost layer and the fin is preferred.

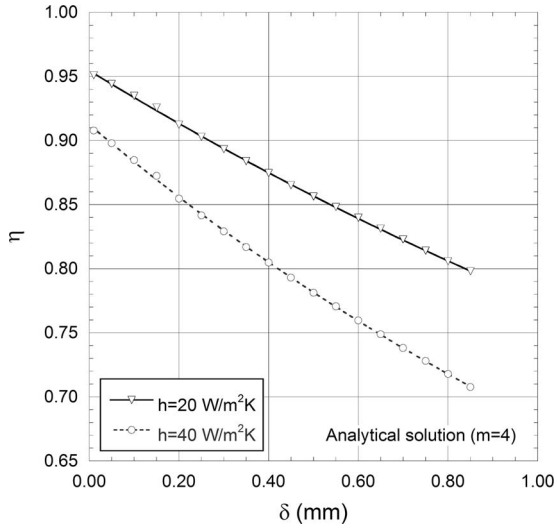

Fig. 3 Using the conditions of Table 1, example fin efficiencies are shown for two values of the convective heat transfer coefficient over a range of frost thicknesses. The effect of neglecting conduction through the frost layer is clearly seen.

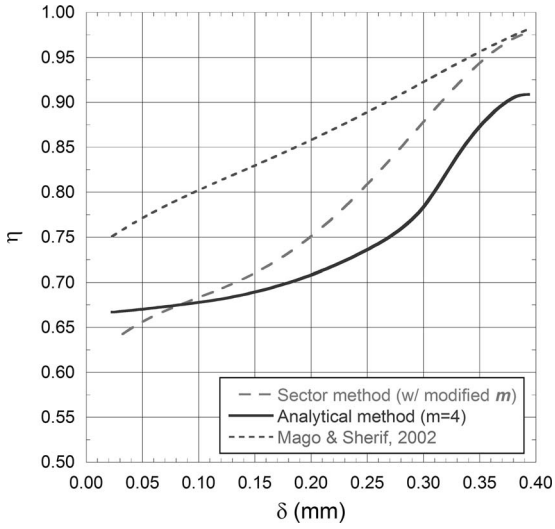

Fig. 4 Using the data from Table 2, the fin efficiency is calculated and shown for different methods and compared to the analytical solution. Note that the convective heat transfer coefficient is not constant; it decreases with frost thickness.

In Fig. 4, the fin efficiency calculated using data from Table 2 and Eq. (29) is compared to two alternate approaches: that of Wu and Bong [4], where the m term is modified to account for latent effects, and that of Mago and Sherif [6], which uses a graphical approach. It should be noted that while both of these approaches seek to account for the transfer of heat by latent effects, neither includes the effect of conduction through the frost layer. Therefore, the observed difference between these two methods is due predominantly to their method of handling the latent effects. The analytical solution yields fin efficiencies several percent lower than the other two methods and deviates the most for large frost thicknesses. It should be noted that the approach by Mago and Sherif [6] does not use the sector method but instead uses equivalent circular areas and requires interpolation from a graph which does not lend itself easily to numerical programming. Unlike Fig. 3, this plot of fin efficiency is derived from actual measured data.

Table 1 Parameters for an example with fixed h

δ	0 to 1.0 mm
h	20,40 W m^{-2} K^{-1}
k_1	237 W m^{-1} K^{-1}
k_2	0.175 W m^{-1} K^{-1}
t	0.0635 mm
R_1	3.868 mm

(Radius Ratios and Surface Area for Sectors in Zones 1, 4, 5, and 8)		(Radius Ratios and Surface Area for Sectors in Zones 2, 3, 6, and 7)	
RR_1=1.235	S_1=0.3650 mm^2	RR_1=3.105	S_1=3.472 mm^2
RR_2=1.246	S_2=0.3770 mm^2	RR_2=3.109	S_2=3.463 mm^2
RR_3=1.267	S_3=0.3999 mm^2	RR_3=3.119	S_3=3.447 mm^2
RR_4=1.299	S_4=0.4316 mm^2	RR_4=3.133	S_4=3.422 mm^2
RR_5=1.340	S_5=0.4693 mm^2	RR_5=3.152	S_5=3.391 mm^2
RR_6=1.389	S_6=0.5105 mm^2	RR_6=3.175	S_6=3.353 mm^2
RR_7=1.446	S_7=0.5531 mm^2	RR_7=3.202	S_7=3.310 mm^2
RR_8=1.509	S_8=0.5950 mm^2	RR_8=3.234	S_8=3.262 mm^2
RR_9=1.579	S_9=0.6352 mm^2	RR_9=3.269	S_9=3.211 mm^2
RR_{10}=1.654	S_{10}=0.6729 mm^2	RR_{10}=3.307	S_{10}=3.158 mm^2
RR_{11}=1.733	S_{11}=0.7076 mm^2	RR_{11}=3.349	S_{11}=3.102 mm^2
RR_{12}=1.817	S_{12}=0.7393 mm^2	RR_{12}=3.394	S_{12}=3.046 mm^2
RR_{13}=1.903	S_{13}=0.7679 mm^2	RR_{13}=3.442	S_{13}=2.989 mm^2
RR_{14}=1.993	S_{14}=0.7937 mm^2	RR_{14}=3.493	S_{14}=2.932 mm^2

Therefore, the convective heat transfer coefficient is not constant but decreases with the thickness of the frost layer, because the air flow rate through the heat exchanger decreases as frost accumulates on the air-side surface.

One-Term Approximation

Because the complete series solution is cumbersome, it is desirable to identify cases for which a one-term approximation to the series solution is sufficient. In order to make such an assessment, consider the eigencondition

$$\tan^{-1}(\beta_m) = \frac{k_1 k_2 t}{\delta(k_2^2 + h k_1 t)}\left[\left(\frac{h\delta^2}{k_1 t}\right)\frac{1}{\beta_m} - \beta_m\right] \tag{30}$$

From Xia and Jacobi [1], the following is known about the first eigenvalue

$$0 < \beta_1 < \sqrt{\frac{h\delta^2}{k_1 t}} \tag{31}$$

Therefore, when

$$\sqrt{\frac{h\delta^2}{k_1 t}} \ll 1 \tag{32}$$

we have $\tan(\beta_m) \approx \beta_m$, and the first root of Eq. (19) can be approximated as

Table 2 Parameters for an example with varying h

δ (mm)	h_{sens} (W m^{-2} K^{-1})	h_{eff} (W m^{-2} K^{-1})	k_1 (W m^{-1} K^{-1})	k_2 (W m^{-1} K^{-1})
0.02	180	218	237	0.40
0.06	156	197	237	0.32
0.14	124	150	237	0.23
0.23	75.9	97.2	237	0.19
0.30	41.4	61.0	237	0.18
0.34	17.6	27.8	237	0.18
0.37	9.5	16.7	237	0.19
0.38	7.3	13.0	237	0.19
0.39	6.5	12.3	237	0.20

$$\beta_1 \approx \delta \sqrt{\frac{h}{k_1 t + \delta\left(\frac{k_1 h t}{k_2} + k_2\right)}} \tag{33}$$

Furthermore, it can be shown from Eq. (30) that when

$$\frac{k_1 k_2 t}{\delta(k_2^2 + h k_1 t)} \gg 1 \tag{34}$$

we can approximate $\sin(\beta_m) \to \beta_m$ and $\cos(\beta_m) \to 1$. Therefore, Eqs. (26*a*)–(26*d*) reduce to

$$C_1 \approx \frac{\left(\frac{\delta}{R_2}\right) \cdot \left(\frac{k_1 t}{\delta^2 h} + \frac{k_2}{h\delta} + \frac{k_1 t}{k_2 \delta}\right)}{\left[K_0\left(\gamma_1 \frac{R_1}{R_2}\right) I_1(\gamma_1) + K_1(\gamma_1) I_0\left(\gamma_1 \frac{R_1}{R_2}\right)\right] \cdot \left[\frac{\beta_1^2 k_2}{h\delta} + \left(\frac{\beta_1 k_2}{h\delta}\right)^2 + \frac{k_1 t}{h^2 \delta^3 k_2}(k_2 \beta_1 + h\delta\beta_1)^2\right]} \tag{35}$$

The one-term approximation to the series solution in the frost layer is then

$$\frac{T_2(r,z) - T_\infty}{T_b - T_\infty} \approx \frac{\beta_1 \cdot \left(\frac{k_1 t}{\delta^2 h} + \frac{k_2}{h\delta} + \frac{k_1 t}{k_2 \delta}\right)}{\left[\frac{\beta_1^2 k_2}{h\delta} + \left(\frac{\beta_1 k_2}{h\delta}\right)^2 + \frac{k_1 t}{h^2 \delta^3 k_2}(k_2 \beta_1 + h\delta\beta_1)^2\right]} \cdot \left[\beta_1 \left(\frac{k_2}{h\delta}\right) \cos\beta_1\left(1 - \frac{z}{\delta}\right) + \sin\beta_1\left(1 - \frac{z}{\delta}\right)\right] \cdot \frac{\left[K_0\left(\beta_1 \frac{r}{\delta}\right) I_1\left(\beta_1 \frac{R_2}{\delta}\right) + K_1\left(\beta_1 \frac{R_2}{\delta}\right) I_0\left(\beta_1 \frac{r}{\delta}\right)\right]}{\left[K_0\left(\beta_1 \frac{R_1}{\delta}\right) I_1\left(\beta_1 \frac{R_2}{\delta}\right) + K_1\left(\beta_1 \frac{R_2}{\delta}\right) I_0\left(\beta_1 \frac{R_1}{\delta}\right)\right]} \tag{36}$$

and in material 1,

$$\frac{T_1(r) - T_\infty}{T_b - T_\infty} \approx \frac{\beta_1 \cdot \left(\frac{k_1 t}{\delta^2 h} + \frac{k_2}{h\delta} + \frac{k_1 t}{k_2 \delta}\right)}{\left[\frac{\beta_1^2 k_2}{h\delta} + \left(\frac{\beta_1 k_2}{h\delta}\right)^2 + \frac{k_1 t}{h^2 \delta^3 k_2}(k_2 \beta_1 + h\delta\beta_1)^2\right]} \cdot \left[\beta_1 \left(\frac{k_2}{h\delta}\right) \cos\beta_1 + \sin\beta_1\right] \cdot \frac{\left[K_0\left(\beta_1 \frac{r}{\delta}\right) I_1\left(\beta_1 \frac{R_2}{\delta}\right) + K_1\left(\beta_1 \frac{R_2}{\delta}\right) I_0\left(\beta_1 \frac{r}{\delta}\right)\right]}{\left[K_0\left(\beta_1 \frac{R_1}{\delta}\right) I_1\left(\beta_1 \frac{R_2}{\delta}\right) + K_1\left(\beta_1 \frac{R_2}{\delta}\right) I_0\left(\beta_1 \frac{R_1}{\delta}\right)\right]} \tag{37}$$

where β_1 is given by Eq. (33). Under the one-term approximation, the fin efficiency is

$$\eta' = \frac{2R_1}{(R_2^2 - R_1^2)h} \cdot \left(\frac{\beta_1^2}{\delta}\right) \cdot \frac{\frac{k_1 t}{\delta^2 h} + \frac{k_2}{h\delta} + \frac{k_1 t}{k_2 \delta}}{\left[\frac{\beta_1^2 k_2}{h\delta} + \left(\frac{\beta_1 k_2}{h\delta}\right)^2 + \frac{k_1 t}{h^2 \delta^3 k_2}(k_2 \beta_1 + h\delta\beta_1)^2\right]} \cdot \frac{\left[K_1\left(\beta_1 \frac{R_1}{\delta}\right) I_1\left(\beta_1 \frac{R_2}{\delta}\right) - K_1\left(\beta_1 \frac{R_2}{\delta}\right) I_1\left(\beta_1 \frac{R_1}{\delta}\right)\right]}{\left[K_0\left(\beta_1 \frac{R_1}{\delta}\right) I_1\left(\beta_1 \frac{R_2}{\delta}\right) + K_1\left(\beta_1 \frac{R_2}{\delta}\right) I_0\left(\beta_1 \frac{R_1}{\delta}\right)\right]} \cdot \left\{k_1 t \beta_1 \left(\frac{k_2}{h\delta}\right) \cos\beta_1 + k_1 t \sin\beta_1 + \frac{k_2 \delta^2}{\beta_1} + \frac{k_2^2 \delta}{h} \sin\beta_1 - \frac{k_2 \delta^2}{\beta_1} \cos\beta_1\right\} \tag{38}$$

It should be noted that while the series solution is completely intractable apart from the use of a computer, the one-term approximation is solvable on almost any hand-held calculator. In Fig. 5, the difference between η and η' is shown as a function of the frost thickness for the conditions given in Table 1. The one-term approximation over-estimates the fin efficiency by up to a few percent at the lowest fin efficiency. For fin efficiencies greater than 75%, the incurred penalty of using the one-term approximation over the series solution (m=4), Eqs. (38) and (29), respectively, is less than 2.3%.

Modifying the Heat Transfer Coefficient

Because the heat transfer in this problem is occurring by both sensible and latent modes of transport, the sensible convective coefficient, h, should be modified to include the latent transfer of heat. In this way, the mass transfer effects are accounted for in a modified air-side convective heat transfer coefficient, for the purpose of calculating fin efficiency. The effective heat transfer coefficient in this case is defined as

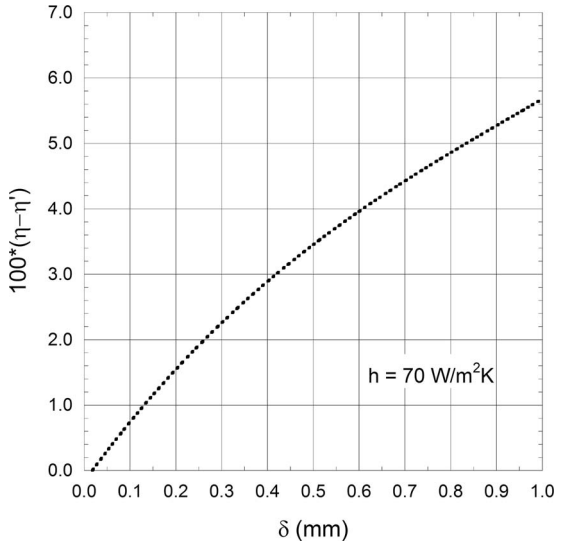

Fig. 5 The difference between the series solution and the one-term approximation is shown using the conditions of Table 1

$$h_{\text{eff}} = \left(h + \frac{Q_{\text{latent}}}{Q_{\text{sensible}}}h\right) = h + \frac{\dot{m}_f i_f}{A_{\text{tot}}\Delta T_{\text{lm},s}} \tag{39}$$

where $\dot{m}_f$ represents the mass deposition rate of the frost, i_f is the ablimation energy, and A_{tot} is the heat exchanger total surface area. In this definition, $\Delta T_{\text{lm},s}$ represents the log-mean temperature difference between the air-stream temperature and the frost surface temperature and is defined as

$$\Delta T_{\text{lm},s} = \frac{(T_{a,\text{up}} - T_f) - (T_{a,\text{down}} - T_f)}{\ln[(T_{a,\text{up}} - T_f)/(T_{a,\text{down}} - T_f)]} \tag{40}$$

This effective heat transfer coefficient should be used in place of h in the above equations. The effect of using this modified heat transfer coefficient is small, but it can lower the fin efficiency by 2.3%–5.3% as shown in Fig. 6, which was based on the data of Table 2. It should be pointed out that the idea of using a modified heat transfer coefficient has already been suggested in the literature. For example, Lin et al. [8] purport this idea in their work on the effect of inlet relative humidity on wet fin efficiency but define their modified convective coefficient using a linear temperature difference. All the results presented earlier were based on the effective heat transfer coefficient described above.

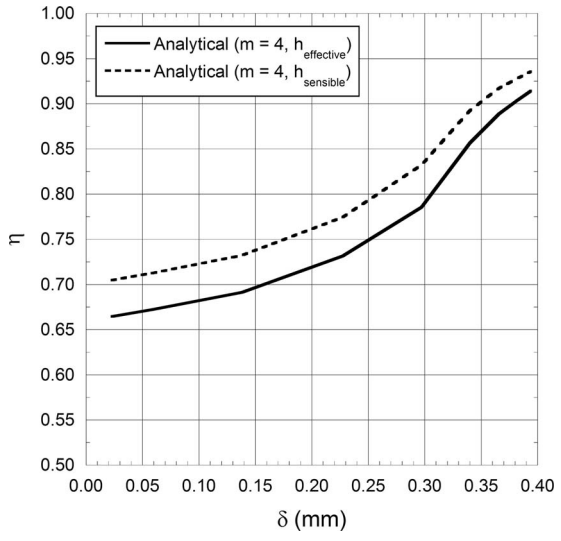

Fig. 6 The difference between using the sensible heat transfer coefficient and the modified convective coefficient in the calculations is shown using the data from Table 2. Note that the convective heat transfer coefficient is not constant; it decreases with frost thickness.

Conclusions

The fin efficiency for a two-dimensional frost layer on a one-dimensional fin has been presented. An exact solution was obtained by separation of variables exploiting an unusual orthogonality condition. Unlike previous solutions for frosted-fin efficiency, this new solution accounts for two-dimensional conduction in the frost layer and necessitates fewer simplifying assumptions. It was demonstrated that even when mass transfer effects are lumped into the air-side convective coefficient, neglecting the frost conduction resistance may result in an overestimate of the fin efficiency by several percent. Conditions are also developed under which a one-term approximation to the solution is sufficient. The analytical solution presented in this paper, and the one-term approximation, have broad applicability in addition to their use for calculating fin efficiency of frost-coated fins.

Acknowledgment

We are grateful for financial support from the Air Conditioning and Refrigeration Center (ACRC) at the University of Illinois.

Appendix

Sector Method for Plain-Fin Geometries. The radius ratio, RR_n, and the surface area of each sector, S_n, are calculated as follows:

Sectors with constant M edge (in Fig. 1, zones 2, 3, 6, and 7)

$$\text{RR}_n = \frac{M}{r_{if}}\sqrt{\left(\frac{2n-1}{2N}\right)^2 + \left(\frac{L}{M}\right)^2}$$

$$S_n = \frac{r_{if}^2}{2}(\text{RR}_n^2 - 1)\left[\tan^{-1}\left(\frac{nM}{NL}\right) - \tan^{-1}\left(\frac{(n-1)M}{NL}\right)\right]$$

where $r_{if}=(D_{ot}+2t)/2$ is the inner radius corrected for fins with collars touching the adjacent fin and $n=1,2,3,\ldots$. N is the number of sectors in each zone.

Sectors with constant L edge (in Fig. 1, zones 1, 4, 5, and 8)

$$\text{RR}_n = \frac{M}{r_{if}}\sqrt{\left(\frac{2n-1}{2N}\right)^2\left(\frac{L}{M}\right)^2 + 1}$$

$$S_n = \frac{r_{if}^2}{2}(\text{RR}_n^2 - 1)\left[\tan^{-1}\left(\frac{nL}{NM}\right) - \tan^{-1}\left(\frac{(n-1)L}{NM}\right)\right]$$

where $M=S_T/2$ and $L=S_L/2$.

The total efficiency is then the sum of the multiplication of the appropriate fin efficiency and S_n for each sector in each zone divided by the sum of the surface area for all sectors in each zone

$$\eta_f = \frac{\sum_{n=1}^{N} S_n \eta_n}{\sum_{n=1}^{N} S_n}$$

again where $n=1,2,3,\ldots$. N is the number of sectors in a zone.

Sector Method for Slit-Fin Geometries. For heat exchangers with slit fins, the radius ratio RR_n has been modified to better estimate the fin efficiency. For these surfaces, the constant M edge is replaced by a constant M_s edge, and the L edge is replaced by a constant L_s edge. Since the accurate calculation of the inner radius is particularly complicated for these geometries, the height of the slits is simply added to the sectors of constant M_s edge, and dividing sectors are assumed as before. (Note: The surface area and radius ratio for the sectors of constant L_s edge are calculated in the same manner as the plain fin heat exchanger.) *Sectors with*

constant M_s edge (in Fig. 1, zones 2, 3, 6, and 7)

$$\mathrm{RR}_n = \frac{\left(M_s \sqrt{\left(\frac{2n-1}{2N} \right)^2 + \left(\frac{L}{M} \right)^2} \right) + h_s}{r_{if}}$$

where $n = 1, 2, 3, \ldots$. N is the number of sectors in each zone and h_s is the height of the slits as measured directly from the fin surface.

Nomenclature

A = heat exchanger surface area (m^2)
Bi = Biot number, $h\delta/k_2\ (1+\psi)$
h = convective heat transfer coefficient ($W\ m^{-2}\ K$)
i = enthalpy of ablimation ($J\ kg^{-1}$)
k = thermal conductivity ($W\ m^{-1}\ K$)
$\dot{m}$ = mass deposition rate ($kg\ s^{-1}$)
M = dimensionless group, R_2/δ
N = dimensionless group defined in Eq. (15*b*)
R_1 = tube radius, see Fig. 2 (m)
R_2 = fin radius; half the distance between tubes, see Fig. 2 (m)
t = half fin thickness, see Fig. 2 (m)
T = temperature (K)

Greek Symbols

β = eigenvalue satisfying Eq. (19)
δ = frost thickness (m)
ϵ = a small parameter, see Eq. (7*e*)
γ = modified eigenvalue, $M\beta$
η = fin efficiency, see Eq. (29)
η' = fin efficiency approximation, from a one-term approximation, see Eq. (38)
ψ = ratio of transverse thermal conduction resistances, $tk_2/\delta k_1$

Subscripts and Superscripts

1 = in the material of the fin
2 = in the material of the frost
a = of the air stream
b = at the fin base
eff = effective
f = frost
lm = log-mean difference
s = at the frost surface
tot = total
∞ = in the environment

References

[1] Xia, Y., and Jacobi, A. M., 2004, "An Exact Solution to Steady Heat Conduction in a Two-Dimensional Slab on a One-Dimensional Fin: Application to Frosted Heat Exchangers," Int. J. Heat Mass Transfer, **47**, pp. 3317–3326.
[2] Schmidt, T. E., 1949, "Heat Transfer Calculations for Extended Surfaces," Refrig. Eng., **57**, pp. 351–357.
[3] McQuiston, F. C., 1975, "Fin Efficiency With Combined Heat and Mass Transfer," ASHRAE Trans., **81**, pp. 350–355.
[4] Wu, G., and Bong, T. Y., 1994, "Overall Efficiency of a Straight Fin With Combined Heat and Mass Transfer," ASHRAE Trans., **100**(1), pp. 367–374.
[5] Hong, K. T., and Webb, R. L., 1996, "Calculation of Fin Efficiency for Wet and Dry Fins," HVAC&R Res., **2**(1), pp. 27–41.
[6] Mago, P. J., and Sherif, S. A., 2002, "Modeling the Cooling Process Path of a Dehumidifying Coil Under Frosting Conditions," J. Heat Transfer, **124**(6), pp. 1182–1191.
[7] Kondepudi, S. N., and O'Neal, D. L., 1993, "A Simplified Model of Pin Fin Heat Exchangers Under Frosting Conditions," ASHRAE Trans., **99**(1), pp. 754–761.
[8] Lin, Y.-T., Hsu, K.-C., Chang, Y.-J., and Wang, C.-C., 2001, "Performance of Rectangular Fin in Wet Conditions: Visualization and Wet Fin Efficiency," J. Heat Transfer, **123**(5), pp. 827–836.
[9] Kim, G. J., and Jacobi, A. M., 1999, "Condensate Accumulation Effects on the Air-Side Thermal Performance of Slit-Fin Surfaces," M.S. thesis, University of Illinois at Urbana-Champaign, IL.